Microstructures and Magnetism of Different Oxides Separating FePt Grains via Ion-Beam Bombardment and Annealing

An-Cheng Sun, Hsun-Feng Hsu[1], Yi-Jing Wu[1], Yi-Lun Chiu[1], Jen-Hwa Hsu[2], Philip W. T. Pong[3], Takao Suzuki[4], and Ko-Wei Lin[1]*

Department of Chemical Engineering and Materials Science, Yuan Ze University, Chungli 320, Taiwan
[1]*Department of Materials Science and Engineering, National Chung Hsing University, Taichung 402, Taiwan*
[2]*Department of Physics, National Taiwan University, Taipei 106, Taiwan*
[3]*Department of Electrical and Electronic Engineering, The University of Hong Kong, Hong Kong*
[4]*MINT Center, University of Alabama, Tuscaloosa, AL 35487, U.S.A.*

Received April 20, 2010; revised August 13, 2010; accepted September 3, 2010; published online December 20, 2010

The effects of the fabrication methods and different capped oxide (SiO_2 and TiO_2) layers on the microstructure and magnetism of FePt thin films were studied. Both structural ordering ($S \sim 0.7$) from the fcc FePt phase to the fct FePt phase and magnetic hardening were observed in the annealed FePt/SiO_2 thin films with a low substrate rotation speed (S_r = 1 rpm). However, only the annealed FePt/SiO_2 thin films prepared with a high S_r (10 rpm) exhibited isolated FePt grains separated by the grain boundary SiO_2, as revealed by transmission electron microscopy and magnetometry. Furthermore, similar results in microstructures and magnetic properties were obtained after replacing the capped layer with TiO_2. However, an enhanced order parameter ($S \sim 0.85$) and a smaller FePt grain size (∼6.8 nm), which are promising characteristics for ultrahigh-density magnetic recording, were achieved in the annealed FePt/TiO_2 thin films; however, the annealed FePt/SiO_2 thin films exhibited a larger grain size (∼15 nm). This indicates that TiO_2 inhibits the grain growth of FePt more effectively than SiO_2.
© 2010 The Japan Society of Applied Physics

DOI: 10.1143/JJAP.49.123001

1. Introduction

(001)-oriented FePt thin films have been considered as one of the most promising candidates for application in future ultrahigh-density perpendicular recording media.[1–7] In order to fulfill this application, it is necessary to fabricate decoupled grains with chemically ordered FePt structures at low temperatures.[8] For example, different oxides such as SiO_2,[9] TiO_2,[7] and Ta_2O_5[10] were added to FePt films to control the grain size effectively. Our previous work[11] demonstrated that FePt grain separation can be achieved by incorporating different amounts of oxygen using an ion-beam deposition technique. In this paper, FePt/TiO_2 thin films with an enhanced order parameter ($S \sim 0.85$) as well as reduced grain sizes (∼6.8 nm) (compared with annealed FePt/SiO_2 thin films) after annealing were reported.

2. Experimental Procedure

Cosputtered FePt films with different substrate rotation speeds ($S_r = 1$ and 10 rpm) on SiO_2 substrates were prepared using a ultrahigh-vacuum (UHV) magnetron sputtering system[9] while a capping SiO_2 or TiO_2 layer was prepared using a dual ion-beam deposition technique.[12,13] Samples were annealed at temperatures ranging from 300 to 700 °C for 10 min in a UHV chamber. No external field was applied during deposition. The crystal structures of the FePt/SiO_2 (or TiO_2) thin films were characterized by grazing angle (1°) X-ray diffraction (XRD) analysis using a Bruker D8 SSS diffractometer (Cu Kα radiation). A JEOL JEM-2010 transmission electron microscopy (TEM) system operating at 200 kV was used for the microstructural analysis. The depth profile of the FePt/SiO_2 thin films was measured using a PHI 5000 VersaProbe/Scanning ESCA microprobe. The room-temperature magnetic measurements were performed in a commercial vibrating sample magnetometer (VSM; Lake Shore 7407) with a maximum magnetic field of 20 kOe. Magnetic domain characterization was carried out using a commercial magnetic force microscopy (MFM) system with a Co-coated tip measured in the remanence state.

3. Results and Discussion

The as-deposited FePt (20 nm)/SiO_2 (15 nm) thin film (substrate rotation speed: 1 rpm) exhibited an fcc FePt phase with a lattice constant of $a \sim 3.81$ Å, as indexed by a preferred (111) orientation of FePt structures in Fig. 1(a) determined by XRD analysis. The same (111) reflections of disordered FePt structures were observed at $2\theta \sim 41°$ for films annealed at 300 °C for 10 min, indicating that the onset of structural phase transformation occurs above 300 °C. However, further increasing the annealing temperatures from 400 to 700 °C resulted in structural phase transformation from fcc FePt to fct FePt ($a \sim 3.84$ Å, $c \sim 3.73$ Å). This is evidenced by the increased intensities of ordered FePt phases such as (001), (110), (002) reflections in Fig. 1(a) and confirmed by the peak shift of (111) reflections from fcc ($2\theta \sim 41°$) to fct ($2\theta \sim 41.5°$) in Fig. 1(b). The order parameters[14] of these annealed FePt/SiO_2 thin films [Fig. 1(c)] were determined to be $S \sim 0.6$, similar to those obtained in our previous results.[11] This indicates that ordered FePt structures were achieved by alternate Fe and Pt deposition via annealing processes. The effect of the capped SiO_2 layer on the separation of FePt grains is discussed below.

To understand the morphology and distribution of SiO_2 in the ordered FePt phases, TEM was used to characterize the FePt (20 nm)/SiO_2 (15 nm) thin films [cross-sectional TEM image shown in the inset of Fig. 2(a)] and the results are shown in Fig. 2. The as-deposited FePt/SiO_2 thin films [Fig. 2(b)] exhibited polycrystalline grains (from 5 to 10 nm in size) of the fcc FePt, bcc Fe, and fcc Pt phases, as characterized by the electron diffraction patterns displayed in the inset of Fig. 2(b). The Fe and Pt structures formed are attributed to the low substrate rotation speed and they strongly inhibit the top SiO_2 layer from diffusing into the

*E-mail address: kwlin@dragon.nchu.edu.tw

 © 2010 The Japan Society of Applied Physics

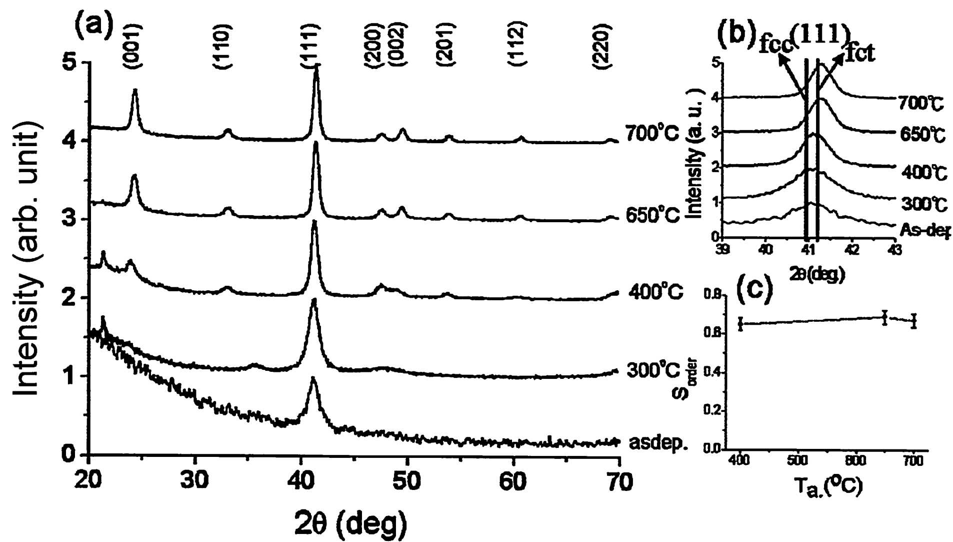

Fig. 1. (a) XRD patterns of FePt/SiO_2 thin films annealed at different temperatures. (b) (111) peak shift from fcc FePt phase to fct FePt phase due to annealing. The order parameter (S) as a function of annealing temperature in annealed FePt/SiO_2 thin films is shown in (c).

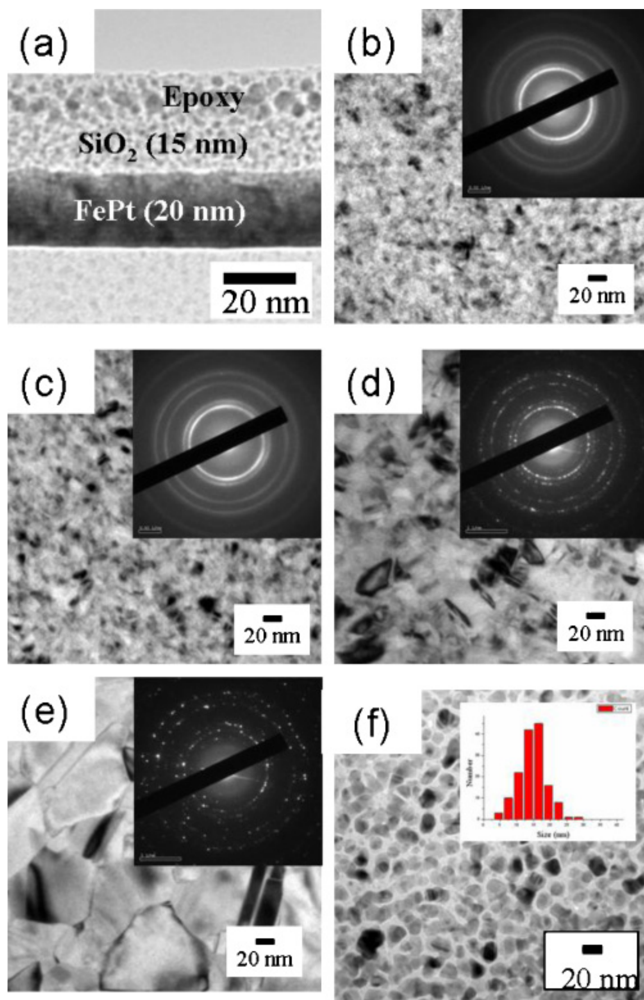

Fig. 2. (Color online) (a) Cross-sectional TEM image of the as-deposited FePt (20 nm)/SiO_2 (15 nm) thin film (S_r = 1 rpm). The corresponding planar-view TEM image and electron diffraction patterns are shown in (b). Similar micrographs of FePt/SiO_2 thin films annealed at different temperatures for 10 min are shown in (c) 300, (d) 400, and (e) 700 °C. The FePt/SiO_2 thin films annealed at 550 °C (S_r = 10 rpm) exhibiting isolated grains are shown in (f). The grain size distribution is shown in the inset of (f).

bottom FePt layer. Similar morphology and structures [Fig. 2(c)] were found for the films annealed at 300 °C, which is in agreement with the XRD results in Fig. 1. In contrast, significant grain growth (average grain size ~30 nm) accompanied by the formation of fct FePt, were observed in the films annealed at 400 and 700 °C, as shown in Figs. 2(d) and 2(e), respectively. It should be noted that although ordered FePt structures were formed after annealing, these annealed FePt/SiO_2 thin films exhibited moderate order parameters ($S \sim 0.6$), as determined by XRD analysis and TEM. However, no FePt grains separated by the grain boundary SiO_2 were observed in these FePt/SiO_2 thin films, which were prepared at a rotation speed of 1 rpm during the deposition of the Fe and Pt layers. In contrast, as the rotation speed increased from 1 to 10 rpm during the fabrication of the Fe and Pt layers, well-separated FePt grains (averaged grain size ~15 nm) by the grain boundary SiO_2 were observed in the films annealed at 550 °C, as demonstrated in Fig. 2(f). It is likely that at a higher rotation speed (10 rpm), disordered FePt forms preferentially during deposition and this provides a fast-diffusion path for SiO_2 during annealing. However, at a lower rotation speed (1 rpm), the formation of polycrystalline Fe and Pt phases serves as a barrier to SiO_2 and prevents the penetration of Si and oxygen atoms into the bottom FePt layers. This is evidenced by the X-ray photoelectron spectroscopy (XPS) results (Fig. 3). The depth profile of elements of FePt capped with SiO_2 is shown in Fig. 3. It is clear that Si and oxygen atoms cannot diffuse into the bottom FePt layers because the Fe and Pt phases serve as a barrier to prevent the penetration. It is thus concluded that the distribution of FePt grains is strongly affected by the fabrication methods (in our case, the substrate rotation speed during deposition).

In order to correlate the microstructures with magnetism in these annealed FePt/SiO_2 thin films, hysteresis loops were measured by VSM at room temperature, as shown in Fig. 4. The as-deposited FePt/SiO_2 thin films were magnetically soft ($H_c \sim 30$ Oe), attributed to the disordered fcc FePt phases.[11] However, the width of the out-of-plane

© 2010 The Japan Society of Applied Physics

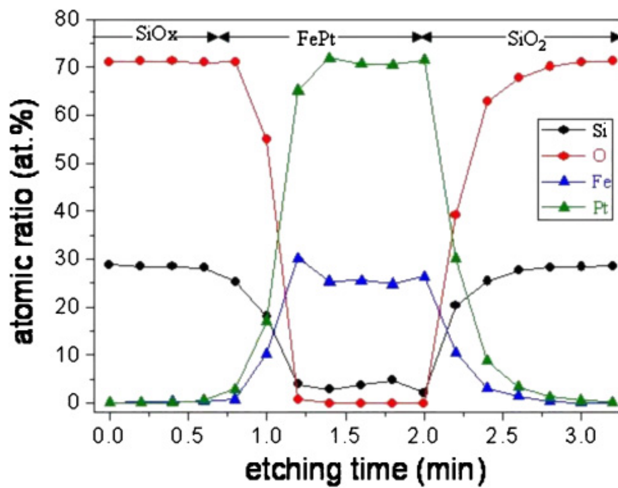

Fig. 3. (Color online) Depth profile of annealed FePt/SiO_2 (550 °C, 10 min) thin films obtained by XPS.

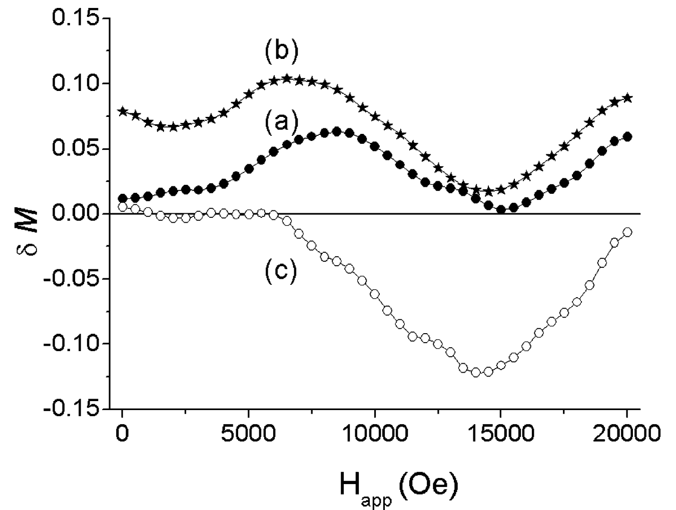

Fig. 5. δM plots of (a) FePt (i.e., without SiO_2 capped layer), (b) FePt/SiO_2 (S_r = 1 rpm), and (c) FePt/SiO_2 (S_r = 10 rpm) thin films annealed at 550 °C for 10 min.

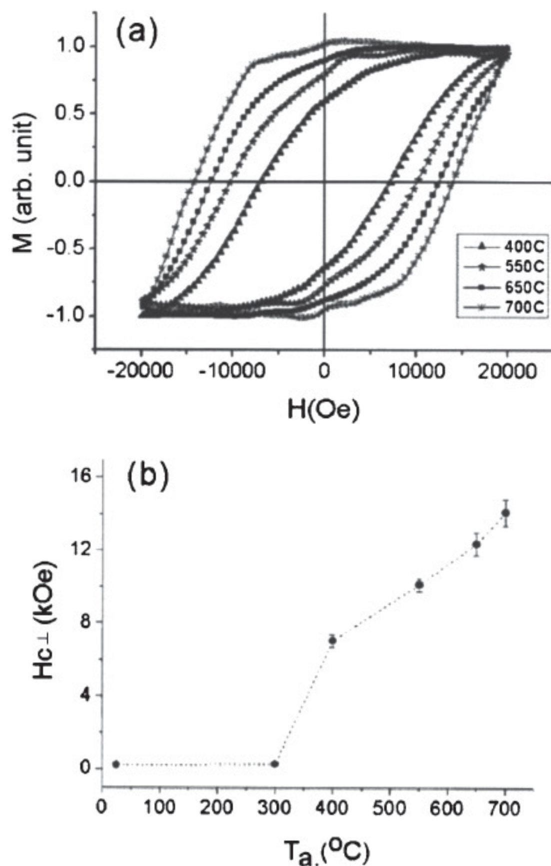

Fig. 4. (a) Out-of-plane hysteresis loops and (b) the dependence of $H_{c\perp}$ on the annealing temperature of the annealed FePt/SiO_2 thin films.

hysteresis loops [Fig. 4(a)] increases with increasing annealing temperature. This indicates that an increasing amount of harder fct FePt phases formed owing to annealing. In addition, the disordered fcc FePt structures characterized by XRD analysis and TEM gives rise to a small $H_{c\perp}$ ($\sim$ 280 Oe) for the films annealed at 300 °C as shown in Fig. 4(b). The onset of a large $H_{c\perp}$ ($\sim$ 7000 Oe) for the films annealed at 400 °C is attributed to the formation of a magnetically hard fct FePt phase. Furthermore, $H_{c\perp}$ increases almost linearly with the annealing temperature with a maximum $H_{c\perp} \sim 14$ kOe obtained for the films annealed at 700 °C. This trend is consistent with the XRD results in Fig. 1(a), which show that the (001) intensity and thus the extent of FePt ordering increase with the annealing temperature.

To characterize the interparticle interactions in recording media and to correlate the results by TEM, a δM [$= M_d - (1 - 2M_r)$, where M_d and M_r represent the reduced dc demagnetization remanence curve and reduced isothermal remanence curve, respectively] plot[15] was constructed, as shown in Fig. 5. It can be seen that without the capped SiO_2 layer, δM shows a positive peak in the annealed FePt thin films ($S_r = 1$ rpm), indicating a strong exchange coupling between FePt grains [Fig. 5(a)]. Even when capped with the SiO_2 layer, the FePt/SiO_2 thin films ($S_r = 1$ rpm) still exhibited a large positive peak in the δM plot, as shown in Fig. 5(b). In contrast, as S_r increases to 10 rpm, a negative peak in the δM plot is observed in the annealed FePt/SiO_2 thin films, as shown in Fig. 5(c). This indicates that the dipolar interparticle interactions[16] existed in the sample. This is consistent with the TEM results [Fig. 2(f)] where the FePt grains are separated by the grain boundary SiO_2.

Since the diffusion length of the oxide into the bottom FePt layers is sensitive to the preparation method, annealing temperature, FePt layer thickness and type of oxide used, an FePt layer of reduced thickness (10 nm) with a different capped layer (TiO_2) was used to form FePt (10 nm)/TiO_2 (10 nm) thin films ($S_r = 10$ rpm), and the films obtained were compared with the FePt/SiO_2 thin films. The magnetic properties and phase structures of the annealed FePt/TiO_2 thin films were determined by VSM and XRD analysis, and the results are shown in Fig. 6. As expected, a marked increase in $H_{c\perp}$ ($\sim$ 3500 Oe) is observed at 400 °C [Fig. 6(a)], indicating a disorder–order (from fcc FePt to fct FePt) structural phase transition is occurring, which is consistent with the XRD pattern in the inset of Fig. 6(a). In addition, significant magnetic hardening resulting from

 © 2010 The Japan Society of Applied Physics

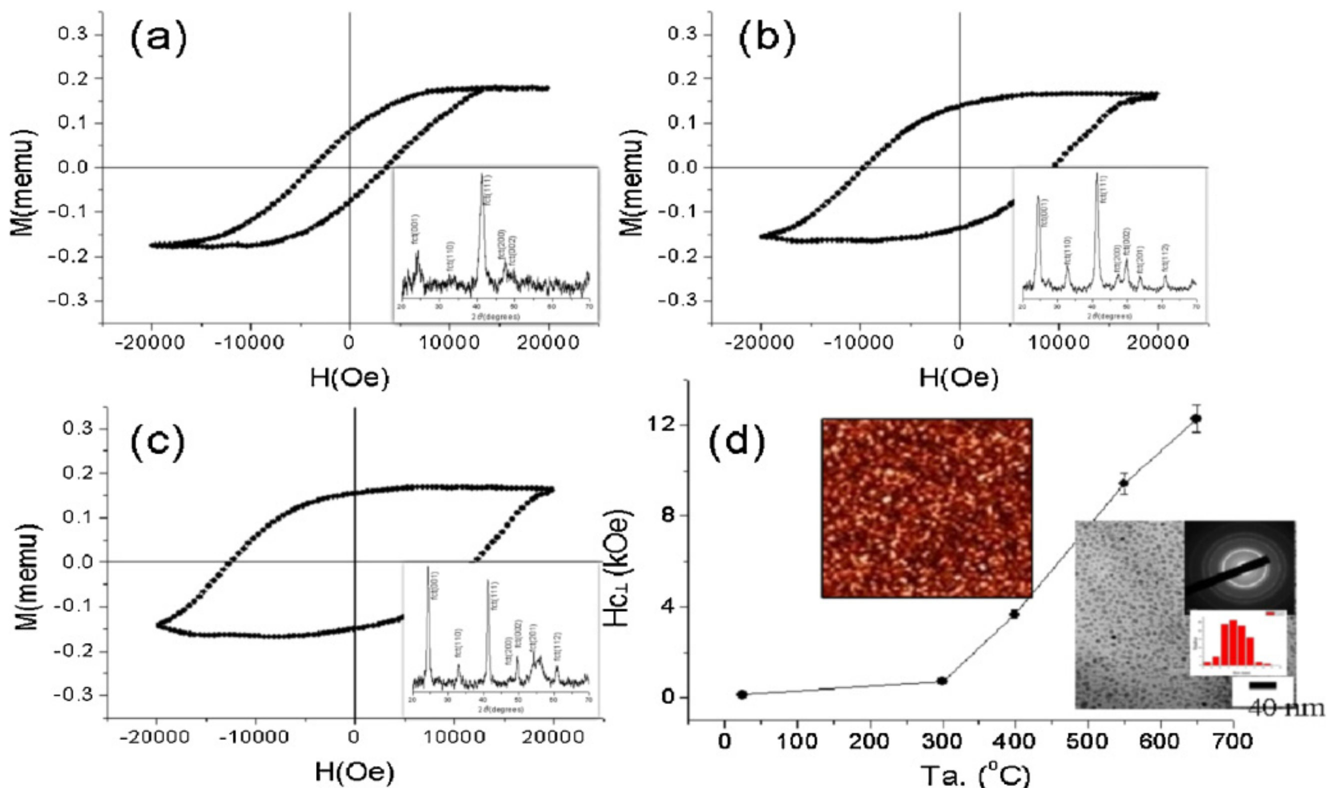

Fig. 6. (Color online) Out-of-plane hysteresis loops of the FePt/TiO_2 thin films annealed at (a) 400, (b) 550, and (c) 650 °C for 10 min; the corresponding XRD patterns are shown in the insets of (a)–(c), respectively. (d) Shows the dependence of $H_{c\perp}$ on the annealing temperature. The planar-view TEM image and MFM image (2 x 2 μm^2) illustrating magnetic domain structures of FePt/TiO_2 thin films (annealed at 550 °C) are shown in the insets of (d).

the FePt ordering (with an enhanced order parameter $S \sim 0.86$ with increasing annealing temperature) is revealed by the expanded out-of-plane hysteresis loops [Figs. 6(b) and 6(c), respectively]. From the XRD patterns in the insets of Figs. 6(b) and 6(c), further increasing the annealing temperature to 550 and 650 °C resulted in a more ordered FePt phase transformation from fcc FePt to fct FePt. This is confirmed by the increased intensities of ordered FePt phases such as (001), (110), (002) reflections, indicating that ordered FePt structures were obtained.

The annealed FePt/TiO_2 thin films exhibited a similar trend of coercivity as a function of annealing temperature as the annealed FePt/SiO_2 thin films [Fig. 2(b)], as shown in Fig. 6(d). The well-separated FePt grains from the grain boundary TiO_2 is shown in the insets of Fig. 6(d) by both the TEM and room-temperature MFM results. It can be observed from the MFM results [inset of Fig. 6(d)] that well-defined magnetic domains are associated with decoupled FePt grains, as opposed to the interconnected domain structures in FePt thin films without SiO_2 addition.[11] The FePt/TiO_2 thin film (annealed at 550 °C) exhibited a reduced grain size (~6.8 nm), smaller than that of the FePt/SiO_2 thin films (~15 nm) [Fig. 2(f)]. The FePt grain size difference between the SiO_2 and TiO_2 capping layers is likely attributed to (1) the surface energy difference and (2) the FePt thickness difference. Our results indicated that, while the surface energy of SiO_2 and TiO_2 is about the same order of magnitude, the reduced FePt thickness from 20 nm (FePt/SiO_2) to 10 nm (FePt/TiO_2) can effectively achieve the grain size refinement and isolate FePt grains. Combining the results of structural, microstructural, and magnetic characterization, it is concluded that by reducing FePt layer thickness and employing a TiO_2 capping layer, a reduced grain size of FePt grains (~6.8 nm) separated by the grain boundary TiO_2 is achieved while maintaining an enhanced order parameter ($S \sim 0.85$) as well as a moderate coercivity (~9000 Oe).

4. Conclusions

The microstructures and magnetic properties of FePt/SiO_2 and FePt/TiO_2 thin films were studied. At low and high substrate rotation speeds, structural ordering (from fcc FePt to fct FePt) and magnetic hardening were observed in FePt/SiO_2 thin films with increasing annealing temperature. However, FePt grains separated by the grain boundary SiO_2 were only observed at a high substrate rotation speed (10 rpm), as evidenced by the TEM images and δM plot. Alternatively, by reducing the FePt layer thickness and replacing the capped layer with Ti oxide, isolated FePt grains separated by the grain boundary TiO_2 were observed in the annealed FePt (10 nm)/TiO_2 (10 nm) thin films. The annealed FePt/TiO_2 thin film exhibited an enhanced order parameter S (~ 0.85), while maintaining a moderate coercivity ($H_{c\perp} \sim 9$ kOe). However, the grain size refinement (~6.8 nm) was achieved in the annealed FePt/TiO_2 thin films, whereas the annealed FePt/SiO_2 thin films had a larger grain size of ~15 nm. Our results indicate that by controlling the fabrication parameters as well as by adding capped oxide layers, small and decoupled FePt grains with good magnetic properties can be obtained.

© 2010 The Japan Society of Applied Physics

Acknowledgments

This work was supported by the Ministry of Economic Affairs of Taiwan (99-EC-17-A-08-S1-006) and by the Seed Funding for Basic Research of the University of Hong Kong.

1) J. Zhu and H. N. Bertram: J. Appl. Phys. **69** (1991) 6084.
2) A. Cebollada, D. Weller, J. Sticht, R. Harp, R. F. C. Farrow, R. F. Marks, R. Savoy, and J. C. Scott: Phys. Rev. B **50** (1994) 3419.
3) M. Watanabe and M. Homma: Jpn. J. Appl. Phys. **35** (1996) 1264.
4) J.-U. Thiele, L. Folks, M. F. Toney, and D. K. Weller: J. Appl. Phys. **84** (1998) 5686.
5) T. Suzuki, N. Honda, and K. Ouchi: J. Appl. Phys. **85** (1999) 4301.
6) C. H. Lai, C. H. Yang, C. C. Chiang, T. Balaji, and T. K. Tseng: Appl. Phys. Lett. **85** (2004) 4430.
7) Y. F. Ding, J. S. Chen, B. C. Lim, J. F. Hu, B. Liu, and G. Ju: Appl. Phys. Lett. **93** (2008) 032506.
8) Y. C. Wu, L. W. Wang, and C. H. Lai: Appl. Phys. Lett. **91** (2007) 072502.
9) A. C. Sun, J.-H. Hsu, P. C. Kuo, and H. L. Huang: J. Magn. Magn. Mater. **320** (2008) 3071.
10) K. M. Pandey, J. S. Chen, G. M. Chow, and J. F. Hu: Appl. Phys. Lett. **94** (2009) 232502.
11) K.-W. Lin, Y.-L. Chiu, A.-C. Sun, J.-H. Hsu, J. van Lierop, and T. Suzuki: Jpn. J. Appl. Phys. **48** (2009) 073002.
12) K.-W. Lin, J.-Y. Guo, S.-R. Lin, H. Ouyang, C.-J. Tsai, J. van Lierop, N. N. Phuoc, and T. Suzuki: Phys. Status Solidi C **4** (2007) 4507.
13) J.-Y. Guo, C.-Y. Liu, H. Ouyang, K.-W. Lin, C.-J. Tsai, J. van Lierop, N. N. Phuoc, and T. Suzuki: Phys. Status Solidi C **4** (2007) 4512.
14) Y. K. Takahashi, T. Koyama, M. Ohnuma, T. Ohkubo, and K. Hono: J. Appl. Phys. **95** (2004) 2690.
15) H. Zeng, S. Sun, T. S. Vengantam, J. P. Liu, Z.-R. Dai, and Z.-L. Wang: Appl. Phys. Lett. **80** (2002) 2583.
16) A. Tomou, I. Panagiotopoulos, D. Gournis, and B. Kooi: J. Appl. Phys. **102** (2007) 023910.

© 2010 The Japan Society of Applied Physics